


ORIGINAL WORK



# Size-Related Differences in Computed Tomography Markers of Hematoma Expansion in Acute Intracerebral Hemorrhage

Yong Soo Kim<sup>1†</sup>, Hee-Yun Chae<sup>1,2†</sup>, Han-Gil Jeong<sup>1,3\*</sup> , Beom Joon Kim<sup>1</sup>, Si-Un Lee<sup>3</sup>, Jihoon Kang<sup>1</sup>, Tackeun Kim<sup>3</sup>, Jae Seung Bang<sup>3</sup>, Hee-Joon Bae<sup>1</sup>, Chang Wan Oh<sup>3</sup> and Moon-Ku Han<sup>1</sup>

© 2021 Springer Science+Business Media, LLC, part of Springer Nature and Neurocritical Care Society

## Abstract

**Background:** Noncontrast computed tomography (NCCT) markers for hematoma expansion (HE) in intracerebral hemorrhage (ICH) are difficult to be found in small ICHs, of which can also expand. We aimed to investigate whether there were size-related differences in the prevalence of NCCT markers and their association with HE.

**Methods:** This retrospective analysis of prospectively collected stroke registry included 267 consecutive patients with ICH who underwent baseline NCCT within 12 h of onset. Qualitative NCCT markers, including heterogeneous density and irregular shape, were assessed. Hematoma density, defined as mean Hounsfield unit of hematoma, and hematoma volume were measured by semiautomated planimetry. Hematoma volume was categorized as small ( $\leq 10$  ml) and large ( $> 10$  ml). Associations of NCCT markers with HE were analyzed using multivariable logistic regression analyses. The model performances of NCCT markers and hematoma density were compared using receiver operating characteristic curves.

**Results:** Hematoma expansion occurred in 29.9% of small ICHs and 35.5% of large ICHs. Qualitative NCCT markers were less frequently observed in small ICHs. Heterogeneous density, irregular shape, and hematoma density were associated with HE in small ICH (adjusted odds ratios [95% confidence interval] 3.94 [1.50–10.81], 4.23 [1.73–10.81], and 0.72 [0.60–0.84], respectively), and hematoma density was also related to HE in large ICH (0.84 [0.73–0.97]). The model performance was significantly improved in small ICHs when hematoma density was added to the baseline model (DeLong's test,  $p = 0.02$ ).

**Conclusions:** The prevalence of NCCT markers and their association with HE differed according to hematoma volume. Quantitative hematoma density was associated with HE, regardless of hematoma size.

**Keywords:** Intracerebral hemorrhage, Hematoma expansion, Computed tomography, Hematoma density

## Introduction

Hematoma expansion (HE) occurs in one third of patients with intracerebral hemorrhage (ICH) [1, 2]. As a major cause of neurologic deterioration and a

potentially modifiable determinant of poor prognosis, HE has emerged as a primary treatment target [3, 4]. Various predictors of HE have been identified, including time from onset to computed tomography (CT) scan, previous administration of antithrombotic drugs, and spot signs [1, 5, 6]. Large baseline hematoma volume is another validated predictor of HE and is known to be related to frequent early neurological worsening and poor outcomes [5]. In addition, diverse neuroimaging and laboratory factors, including presence of

\*Correspondence: han.g.jeong@gmail.com

<sup>†</sup>Yong Soo Kim and Hee-Yun Chae have contributed equally to this work.

<sup>1</sup> Department of Neurology, Seoul National University Bundang Hospital, Seongnam, Republic of Korea

Full list of author information is available at the end of the article

(See figure on next page.)

**Fig. 1** Representative cases of small ICHs with or without NCCT markers. **a** ICH without any qualitative NCCT markers that expanded in follow-up CT scan after 2 h from the baseline scan. Baseline hematoma density (mean HU) was 51.7 HU. **b** ICH with heterogeneous densities (black arrows) that did not expand in follow-up CT scan after 21 h from the baseline scan. Baseline hematoma density (mean HU) was 55.0 HU. **c** ICH with satellite sign (black arrow), blend sign (dashed black arrow), and black hole sign (white arrow) that did not expand in follow-up CT scan after 23 h from the baseline scan. Baseline hematoma density (mean HU) was 58.4 HU. **d** ICH with irregular shape and island sign (black arrows) that did not expand in follow-up CT scan after 10 h from the baseline scan. Baseline hematoma density (mean HU) was 57.1 HU. CT, computed tomography, HU, Hounsfield unit, ICH, intracerebral hemorrhage, NCCT, noncontrast computed tomography

intraventricular hemorrhage, hyperglycemia, and anemia, have also been suggested as predictors of HE and poor outcomes [5, 7, 8].

Noncontrast computed tomography (NCCT) markers, including heterogeneous densities, blend sign, irregular shape, and island sign, are emerging predictors of HE [3, 9–11]. Ongoing bleeding or rebleeding from the initial ruptured vessel and secondary bleeding from damage to the neighboring vessels are known as possible mechanisms of HE, and NCCT markers are accepted as a way to reflect these multifocality and temporal differences in bleeding [3, 9, 12]. Because those markers can be evaluated without intravenous contrast imaging, they are expected to be possible alternatives for CT angiographic spot signs [13, 14]; however, despite good performance for predicting HE, some NCCT markers have shown limited sensitivity and varied incidence between studies [15].

Small ICHs are known to be related to less frequent HE, compared with large ICHs [16]. Accordingly, small ICHs have received little attention because of their self-limited clinical course; however, approximately 20% of small ICHs expand and can cause poor functional outcomes [17–19]. Small ICHs tend to be more regularly shaped and homogenous, whereas large ICHs tend to be irregularly shaped and heterogeneous [3]. To date, it is still unknown whether these characteristics reflect an inherent low risk of HE in small ICHs or a limited spatial resolution of NCCT in evaluating small ICHs [13, 15]. This study aimed to investigate hematoma size-related differences in the prevalence of NCCT markers and their performance in predicting HE.

## Methods

### Patients

We screened 549 consecutive patients with ICH who were admitted to a single tertiary referral hospital from January 2011 to August 2018. Patients who had their first CT scan within 12 h from onset ( $n = 340$ ) and who had at least one follow-up CT scan within 72 h from onset ( $n = 267$ ) were included. This study was approved by the institutional review board of Seoul National

University Bundang Hospital (approval number: B-2011/648–105).

### Clinical Data Collection

Patient characteristics and clinical data were obtained from our prospectively collected stroke registry database, including age, sex, and past medical history (hypertension, diabetes mellitus, hyperlipidemia, atrial fibrillation, and previous intake of antiplatelet agents and anticoagulants). National Institute of Health Stroke Scale score at admission, time last known well, systolic blood pressure at admission, and modified Rankin Scale after 3 months were also assessed.

### Imaging Data Collection and Definition

Noncontrast computed tomography scans were performed with our standard protocols on 64-slice or 128-slice CT scanners (Brilliance 64 and iCT; Phillips Medical Systems, Best, the Netherlands) using an axial technique with 120 kVp, 190–250 mA, and 5-mm slice thickness reconstruction. ICH was defined as an acute neurologic deficit with new intraparenchymal hemorrhage confirmed by CT scan. The timing of follow-up CT scans were dependent on attending physician/care team.

Two trained vascular neurologists (CHY and KYS) who were anonymized to the clinical information and prognosis independently reviewed NCCT scans after the initial training session of 100 patients external to our analysis. Qualitative NCCT markers of HE (heterogeneous density, black hole sign, blend sign, irregular shape, island sign, and satellite sign) were identified with a visual inspection (Fig. 1). Hematomas with heterogeneous density and irregular shape were investigated on the axial NCCT slice that showed the largest hematoma area, according to the shape and density scales suggested by Barras et al. [3, 9] The density and shape scales are two separate 5-point categorical scales, and each scales range from category 1 (regular in shape scale and homogenous in density scale) to category 5 (irregular in shape scale and heterogeneous in density scale). Heterogeneous density and irregular shape was defined as shape and density scale of category 3, 4, or 5. Hematomas with heterogeneous density and irregular shape were defined as shape and density scale of III, IV, or V on the axial

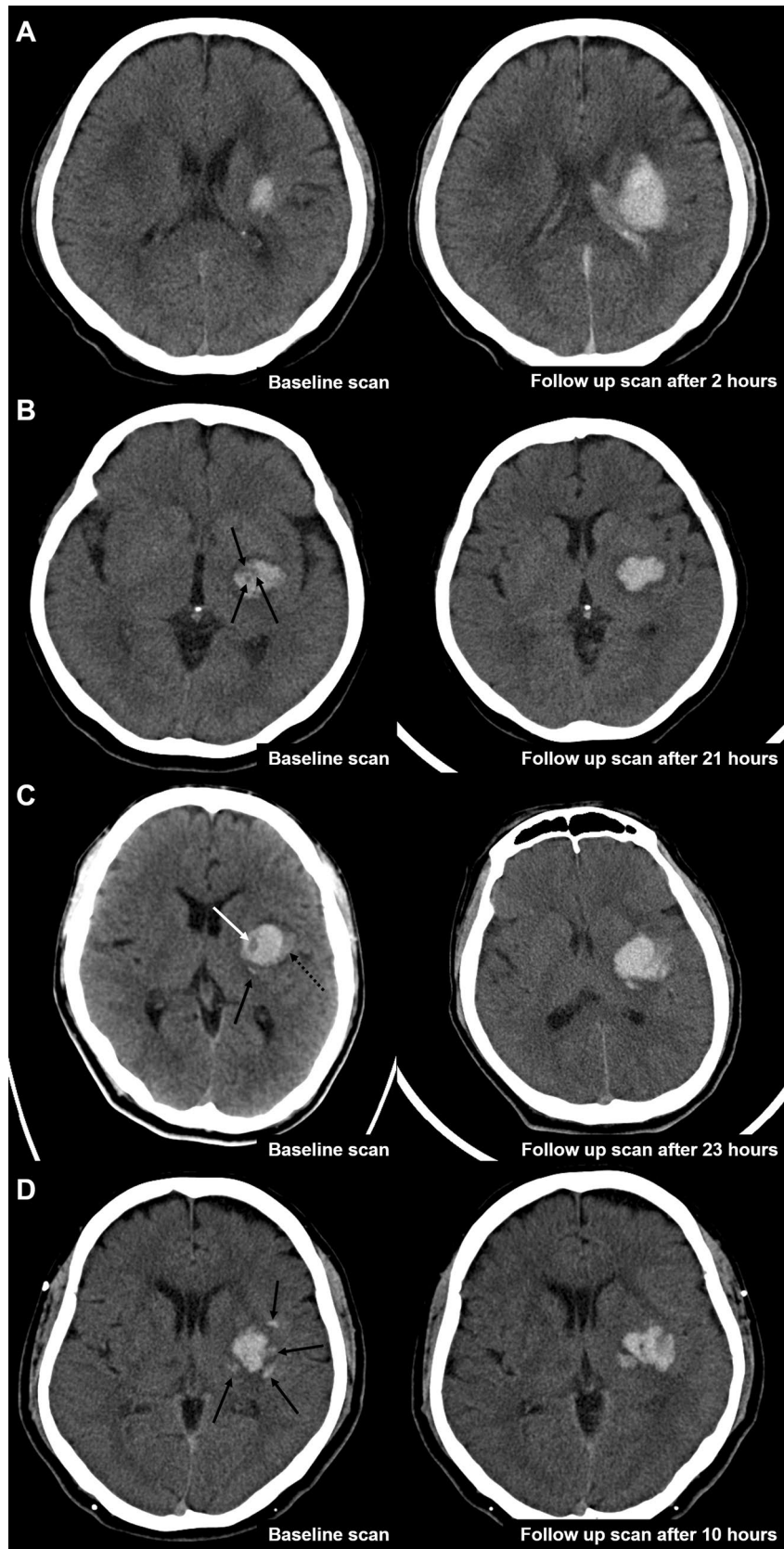


Fig. 1 (See legend on previous page.)

NCCT slice showing the largest hematoma area as Baras et al. suggested [3, 9]. Black hole sign was defined as relatively hypoattenuated lesion, with a density difference at least 28 Hounsfield units (HU) compared with surrounding hematoma [20]. The definition of blend sign was coexistence of well demarcated hypodensity lesion and hyperdensity lesion with density difference of more than 18 HU [10]. Island sign was referred to as the presence of  $\geq 3$  small hematomas completely separated or  $\geq 4$  small hematomas partly separated from the main hematoma [11]. Satellite sign was defined as small hematoma ( $\leq 10$  mm) separated from the main hematoma, with distance of 1 to 20 mm on at least one slice of the NCCT scan [21]. Discrepancies between the two readers (17 heterogenous densities, 7 black hole signs, 19 blend signs, 31 irregular shapes, 35 island signs, and 27 satellite signs) were adjudicated by joint discussion until a consensus was reached.

Hematomas with a threshold between 44 and 100 HU were segmented using semiautomated planimetric analysis by Analyze 14.0 (Analyze Direct Inc, Overland Park, KS). Then, hematoma volume and hematoma density, defined as mean HU of hematoma, were calculated. The volume of intraventricular hemorrhage was excluded. The growth of hematoma more than 6 ml or relatively more than 33% compared with the baseline hematoma was defined as HE. Hematoma volumes in all CT scans taken within 72 h from onset were measured and used to define HE. Small ICH was defined as a hematoma volume not exceeding 10 ml; the ICH with a hematoma volume  $\geq 10$  ml was categorized as a large ICH [3, 18, 19].

### Statistical Analysis

Differences between two groups dichotomized by the baseline hematoma volume were analyzed using  $\chi^2$  test for categorical variables and Student's *t*-tests for continuous variables. The interobserver agreement for segmentation of NCCT markers was calculated using weighted kappa statistics. Exploratory bivariate analysis was performed to identify differences in patient characteristics and occurrence of HE between small and large ICH groups. Univariable and multivariable logistic regression models were constructed separately in small and large ICH groups to determine the correlation of NCCT predictive markers with occurrence of HE. Age, sex, and previously known HE predictive markers (time from onset to CT, volume of hematoma, and previous use of antithrombotic agents) were used as covariates in multivariable logistic regression analysis [5, 22, 23]. As a post hoc subgroup analysis, we performed the multivariable logistic regression analysis in patients with CT scans obtained within 6 h. Results of logistic regression models were reported as unadjusted and adjusted odds ratios

with 95% confidence intervals (CI). The receiver operating characteristic (ROC) analysis was performed in small and large hematoma groups to compare the value of qualitative NCCT markers and hematoma density (mean HU of hematoma) in predicting HE. The areas under the curves (AUCs) of these predictors were compared by using DeLong's test. In the subgroup with CT angiography, AUC was compared with the AUC of validated HE prediction scores, such as a 9-point score and a PREDICT-B score. A two-sided *p* value of 0.05 was set for the threshold of statistical significance and the 95% CI was reported. R version 4.0.3 (R Development Core Team, Vienna, Austria) was used for all analyses.

### Results

Of the 267 patients included in our study, 88 (33.0%) patients had HE. The median time from onset to detection of HE was 28.7 (interquartile range 11.5–51.5) hours. The number of CT scans taken within 72 h of onset was 2 (2–3) in the small ICH group and 3 (2–3) in the large ICH group. The median time from baseline CT to follow-up CT scan was 14.0 (3.9–24.2) hours at first follow-up, 37.9 (17.4–46.7) hours at second follow-up ( $n=136$ ), 41.5 (25.4–57.2) hours at third follow-up ( $n=41$ ), and 51.6 (41.4–65.6) at fourth follow-up. The median time from onset to HE detection was 28.7 (11.5–51.5) hours. The characteristics of included and excluded patients are compared in Supplemental Table 1.

Based on the volume of ICH, 127 (47.6%) patients presented with small ICHs, and 140 (52.4%) patients had large ICHs (Table 1). Patients with large ICHs had higher National Institute of Health Stroke Scale scores at admission and a longer time from onset to CT scan than those with small ICHs. Basal ganglia and lobar ICHs were more frequent in the large ICH group than in the small ICH group. The characteristics of patients according to the presence of HE was described in Table 2.

NCCT markers, including heterogeneous density, black hole sign, blend sign, irregular shape, island sign, and satellite sign, were more frequently observed in patients with large ICHs (Table 1, all *p* values  $< 0.01$ ). Interobserver agreement for identifying NCCT markers was good between the two readers ( $\kappa$ -values were 0.87 for heterogenous density, 0.91 for black hole sign, 0.79 for blend sign, 0.77 for irregular shape, 0.74 for island sign, 0.80 for satellite sign, and 0.88 for hematoma density). Hematoma density was higher in the large ICH group than that in the small ICH group (*p* value  $< 0.01$ ). In addition, there was no statistical difference between small and large ICH groups in occurrence of HE (29.9% vs. 35.7%, *p* value = 0.38), but the extent of HE was larger in patients with large ICHs. The large ICH group had poorer

**Table 1** Baseline characteristics according to the hematoma volume

	Small ICH (n = 127)	Large ICH (n = 140)	p-values
<i>Demographics</i>			
Age	62.7 ± 12.4	64.0 ± 15.4	0.45
Male sex	80 (63.0%)	87 (62.1%)	0.99
<i>Past medical history</i>			
Hypertension	112 (88.2%)	105 (75.0%)	< 0.01
Diabetes mellitus	32 (25.2%)	26 (18.6%)	0.25
Hyperlipidemia	35 (27.6%)	29 (20.7%)	0.24
Atrial fibrillation	15 (11.8%)	8 (5.7%)	0.12
Prior antithrombotic use	34 (26.8%)	35 (25.0%)	0.85
<i>Clinical information</i>			
Baseline NIHSS score	10 (6 to – 15)	15 (11 to – 21)	< 0.01
Onset to CT time (hours)	1.5 (1.1 to – 3.4)	2.0 (1.3 to – 4.9)	0.04
Systolic BP (mm Hg)	170.1 ± 33.3	173.0 ± 34.9	0.49
Diastolic BP (mm Hg)	94.1 ± 22.2	95.1 ± 22.1	0.72
<i>Imaging information</i>			
Baseline ICH volume (ml)	5.0 ± 3.0	27.4 ± 19.6	< 0.01
ICH location			< 0.01
Basal ganglia	50 (39.4%)	62 (44.3%)	
Thalamus	47 (37.0%)	23 (16.4%)	
Lobar	6 (4.7%)	43 (30.7%)	
Infratentorial	24 (18.9%)	12 (8.6%)	
<i>NCCT markers</i>			
Heterogenous density	29 (22.8%)	88 (62.9%)	< 0.01
Black hole sign	11 (8.7%)	33 (23.6%)	< 0.01
Blend sign	14 (11.0%)	37 (26.4%)	< 0.01
Irregular shape	34 (26.8%)	95 (67.9%)	< 0.01
Island sign	22 (17.3%)	86 (61.4%)	< 0.01
Satellite sign	33 (26.0%)	98 (70.0%)	< 0.01
Hematoma density, mean HU	56.8 ± 3.4	58.9 ± 3.2	< 0.01
Presence of IVH	30 (23.6%)	43 (30.7%)	0.25
<i>Outcomes</i>			
Hematoma expansion	38 (29.9%)	50 (35.7%)	0.38
Maximal volume difference	3.2 ± 7.3	6.8 ± 12.3	< 0.01
3 months mRS (4 to 6)	40 (31.5%)	79 (56.4%)	< 0.01

BP blood pressure, CT computed tomography, HU hounsfield unit, ICH intracerebral hemorrhage, IVH intraventricular hemorrhage, mRS modified rankin scale, NCCT noncontrast computed tomography, NIHSS national institutes of health stroke scale

functional outcomes (modified Rankin Scale 4 to 6) at 3 months after the ICH than that in the small ICH group.

Exploratory bivariate analysis, which was used to determine differences in patient characteristics according to HE, revealed that HE frequently occurred in lobar and infratentorial ICHs in both small and large ICH groups (Supplemental table 2). Baseline volume was related to HE in the large ICH group, but hematoma volume was not significantly different between patients with and without HE in the small ICH group.

Univariable logistic regression analysis showed that heterogeneous density, irregular shape, and hematoma

density were significantly associated with a higher possibility of HE in the small ICH group (Table 3). Multivariable logistic regression analysis showed an identical association between NCCT markers and the possibility of HE after adjusting for covariates, including age, sex, previous administration of antithrombotic agents, baseline hematoma volume, and time from onset to CT. However, in the large ICH group heterogeneous density, blend sign, and hematoma density were associated with HE in univariable analysis, but only hematoma density was statistically related to HE in multivariable analysis. In the subgroup of patients who had CT scans performed

**Table 2 Characteristics of all included patients according to HE**

	Without HE (n = 179)	With HE (n = 88)	p-values
<i>Demographics</i>			
Age	61.7 ± 13.7	66.9 ± 14.2	< 0.01
Male sex	111 (62.0%)	56 (63.6%)	0.90
<i>Past medical history</i>			
Hypertension	143 (79.9%)	74 (84.1%)	0.51
Diabetes mellitus	35 (19.6%)	23 (26.1%)	0.29
Hyperlipidemia	41 (22.9%)	23 (26.1%)	0.67
Atrial fibrillation	13 (7.26%)	10 (11.4%)	0.37
Prior antithrombotic use	43 (24.0%)	26 (29.5%)	0.41
<i>Clinical information</i>			
Baseline NIHSS score	12 (7 to – 17)	15.5 (9.8 to – 21.3)	< 0.01
Onset to CT time (hours)	1.9 (1.3 to – 4.1)	1.6 (1.0 to – 3.4)	0.30
Systolic BP (mm Hg)	174 ± 34.6	167 ± 32.7	0.12
Diastolic BP (mm Hg)	96.2 ± 22.5	91.4 ± 21.1	0.09
<i>Imaging information</i>			
Baseline ICH volume (ml)	14.1 ± 14.3	22.1 ± 23.5	< 0.01
ICH location			< 0.01
Basal ganglia	83 (46.4%)	29 (33.0%)	
Thalamus	57 (31.8%)	13 (14.8%)	
Lobar	22 (12.3%)	27 (30.7%)	
Infratentorial	17 (9.50%)	19 (21.6%)	
<i>NCCT markers</i>			
Heterogenous density	65 (36.3%)	52 (59.1%)	< 0.01
Black hole sign	23 (12.8%)	21 (23.9%)	0.04
Blend sign	26 (14.5%)	25 (28.4%)	0.01
Irregular shape	77 (43.0%)	52 (59.1%)	0.02
Island sign	68 (38.0%)	40 (45.5%)	0.30
Satellite sign	84 (46.9%)	47 (53.4%)	0.39
Hematoma density, mean HU	58.5 ± 3.5	56.7 ± 3.1	< 0.01
Presence of IVH	51 (28.5%)	22 (25.0%)	0.65
<i>Outcomes</i>			
Maximal volume difference	0.8 ± 1.2	13.8 ± 14.5	< 0.01
3 months mRS (4 to 6):	63 (35.2%)	56 (63.6%)	< 0.01

BP blood pressure, NIHSS national institutes of health stroke scale, CT computed tomography, HE hematoma expansion, HU hounsfield unit, ICH intracerebral hemorrhage, IVH intraventricular hemorrhage, NCCT noncontrast computed tomography, mRS modified rankin scale

within 6 h of onset, the association between NCCT markers and HE were similar to the original analysis, except for blend sign (Supplemental Table 3). In small ICH group, the association between hematoma density and HE was insignificant in the multivariable logistic regression analysis, which was adjusted for covariates, and were significant ( $p$  value < 0.10) in the bivariate analysis (post hoc sensitivity analysis, Supplemental Table 4).

The area under the ROC curve of the baseline model including previously known HE predictors (time from onset to CT, previous use of antithrombotic agents, and hematoma volume) in the small hematoma group was 0.62 (95% CI 0.51–0.73; Table 4 and Fig. 2). When

qualitative NCCT markers were added to the model, this model did not perform better than the baseline model, but when hematoma density was added to the baseline model, AUC was improved to 0.77 (95% CI 0.68–0.85), which was significantly different to that in the baseline model (DeLong's test,  $p=0.02$ ) in the small ICH group. When qualitative NCCT markers and hematoma density were added together, the models performed better than the baseline models in the small (DeLong's test,  $p=0.01$ ) and large (DeLong's test,  $p=0.03$ ) ICH groups. The area under the ROC curve value was significantly improved after qualitative NCCT markers and hematoma density were added to the baseline model in models of all ICH.



**Table 3 Univariable and multivariable analyses for associations between NCCT markers and hematoma expansion**

	Unadjusted OR (95% CI)	p-values	Adjusted OR (95% CI)	p-values
<i>Small ICH (n = 127)</i>				
Heterogenous density	3.49 (1.47 to 8.41)	<0.01	3.94 (1.50 to 10.81)	<0.01
Black hole sign	3.15 (0.89 to 111.63)	0.07	3.33 (0.83 to 14.18)	0.09
Blend sign	1.90 (0.58 to 5.90)	0.27	1.73 (0.50 to 5.74)	0.37
Irregular shape	3.43 (1.50 to 7.95)	<0.01	4.23 (1.73 to 10.81)	<0.01
Island sign	1.81 (0.68 to 4.67)	0.22	1.85 (0.67 to 5.04)	0.23
Satellite sign	1.79 (0.77 to 4.12)	0.17	1.90 (0.79 to 4.58)	0.15
Hematoma density, per 1 HU increase	0.82 (0.72 to 0.93)	<0.01	0.72 (0.60 to 0.84)	<0.01
<i>Large ICH (n = 140)</i>				
Heterogenous density	2.18 (1.04 to 4.76)	0.04	1.52 (0.61 to 3.88)	0.37
Black hole sign	1.71 (0.77 to 3.80)	0.18	1.52 (0.60 to 3.80)	0.37
Blend sign	2.45 (1.14 to 5.34)	0.02	2.24 (0.96 to 5.27)	0.06
Irregular shape	1.67 (0.56 to 2.50)	0.69	0.67 (0.28 to 1.60)	0.37
Island sign	1.04 (0.51 to 2.13)	0.92	0.53 (0.23 to 1.21)	0.14
Satellite sign	0.86 (0.41 to 1.85)	0.70	0.62 (0.27 to 1.44)	0.27
Hematoma density, per 1 HU increase	0.83 (0.73 to 0.93)	<0.01	0.84 (0.73 to 0.97)	0.02

Covariates for multivariable model included age, sex, time from onset to CT, volume of hematoma, and previous use of antithrombotic agents

CI confidence interval, CT computed tomography, HU hounsfield unit, ICH intracerebral hemorrhage, NCCT noncontrast computed tomography, OR odds ratio

**Table 4 Comparison of AUROC between various predictive models of HE**

Models	AUROC (95% CI)	
	Small ICH	Large ICH
Model A: Baseline clinical predictors	0.62 (0.51 to 0.73)	0.67 (0.57 to 0.76)
Model B: Model A + qualitative NCCT markers	0.70 (0.59 to 0.80)	0.73 (0.65 to 0.82)
Model C: Model A + hematoma density	0.77 (0.68 to 0.85)	0.74 (0.66 to 0.82)
Model D: Model A + qualitative NCCT markers + hematoma density	0.79 (0.70 to 0.88)	0.78 (0.70 to 0.86)

Baseline clinical predictors included time from onset to CT, previous use of antithrombotic agents, and hematoma volume

AUROC area under the receiver operating characteristics, CI confidence interval, HE hematoma expansion, HU hounsfield units, ICH intracerebral hemorrhage, NCCT noncontrast computed tomography

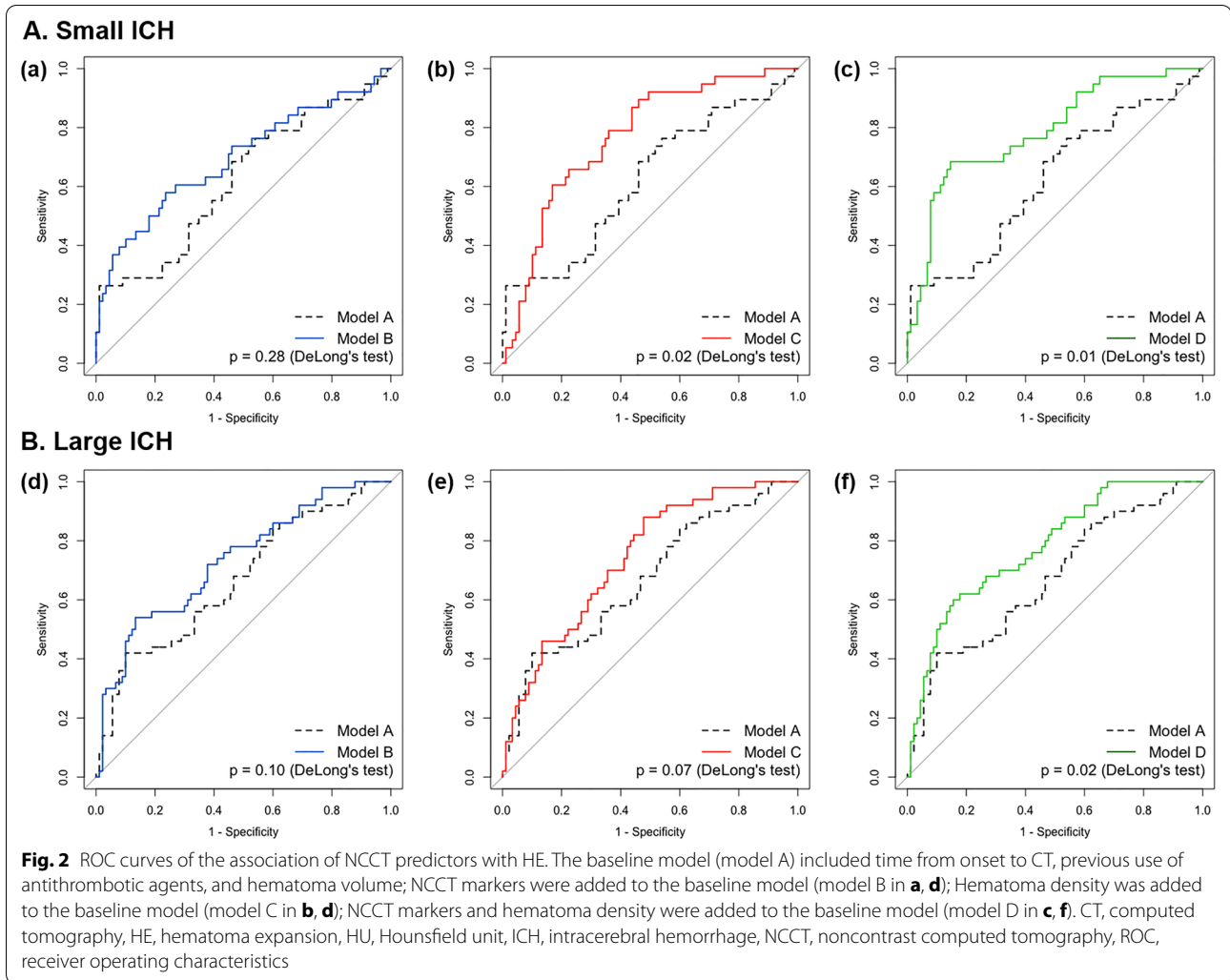
The comparison with the baseline models adjusted with all significant variables are described in Supplemental Table 5. The performance of model, including qualitative NCCT markers and hematoma density, was better than the 9-point score and comparable with the PREDICT-B score (Supplemental Table 6).

## Discussion

Our study demonstrated that the prevalence of NCCT markers and their association with HE were different according to the hematoma size. The NCCT markers predicting HE were less frequently observed in small sized ICHs. In small ICHs, heterogeneous density and irregular shape were significantly associated with HE. Notably, hematoma density was related to HE, regardless of the hematoma size. These findings suggest that the visual inspection of NCCT markers has limited value in predicting HE of small ICHs, whereas hematoma density, a

quantitative measure, may provide additional use. Semi-automatic planimetric method allowed us to measure the volume of hematomas more accurately, define HE more rigorously, and test quantitative hematoma density as a size-independent predictor of HE, compared with the previous studies dealing with the size issues of NCCT markers.

It is well known that the large volume of hematoma is highly associated with HE [2, 5]. HE and prognosis of small ICHs have been less focused because small ICHs are considered to have a low risk of expansion [18]. However, recent studies showed that 26–40% of small ICHs expanded and HE was independently related to early neurological deterioration [17, 19]. Qualitative NCCT markers are considered to reflect the pathophysiology of HE, and they are known to have good specificity in predicting HE; however, they have relatively low sensitivity and low positive predictive



value [9, 15]. In our study, NCCT markers were less frequently observed and only heterogeneous density and irregular shape were associated with HE in small ICHs. Low incidence of NCCT markers in small ICHs was already described before and was supposed to be related to the low possibility of HE [3]. However, it is possible that underdetection of NCCT markers simply because of the small size of ICHs might have contributed to the low sensitivity of NCCT markers in small ICHs that also have potential to expand. Meanwhile, irregular shape, island sign, and satellite sign were associated with lower possibility of HE in large ICHs, although there was no statistical significance. This may have been caused by the high incidences of these qualitative NCCT markers in our study (each 67.9%, 61.4%, and 70.0% among large ICHs), which were inconsistent with previous studies [11, 15].

It is challenging to evaluate the density and shape of the hematoma on NCCT because of image noise,

artifacts, and similar appearance of cerebral parenchyma. Moreover, the current spatial resolution of CT may not be appropriate for grading qualitative density markers precisely, especially in small ICHs. Quantitative density assessments of hematomas when measured semiautomatically, for example, hematoma density in our study, are expected to have good interrater and intrarater reliability and well predict HE, regardless of the size of ICH. Hematoma density is also known to reflect the efficiency of hemostasis within hematoma, as the CT attenuation of hematoma increases in hyperacute phase of bleeding when sufficient hemostasis occurs [24, 25]. This initial increment of CT attenuation largely depends on clot contraction, which is the final step of blood clot maturation. When bleeding occurs, platelets aggregate and build platelet–fibrin network to form the temporary seal [26]. Then, red blood cells embed within the platelet–fibrin network to form a clot [27]. Finally, clot contracts to enhance



the local hemostasis. In this period, because of platelet-generated contractile force, serum is extruded and local concentration of red blood cells within the clot increases [28]. This phenomenon manifests as the increment of hematoma density on CT scan.

Recently, quantitative radiographic features are receiving attention to determine the characteristics of small lesions on medical images, representatively, to differentiate malignant tumors from benign tumors [29]. This emerging approach, also called radiomics, has been applied to predict HE in patients with ICH. For example, Zhan et al. [30] recently revealed that spatial heterogeneity within hematoma represented by quantitative radiomics scores was associated with HE and poor outcomes in small ICHs. The quantitative radiomics scores may supplement visually inspected qualitative NCCT markers, but they may not be suitable when emergent decisions are required. In our study, hematoma density, a quantitative NCCT marker, performed well in predicting HE, regardless of hematoma volume, and showed potential to be used practically and objectively in hyperacute situations. However, these quantitative NCCT features only provide continuous numeric figures; thus, further validation and identification of the cutoff value is necessary. Patients with lower hematoma density than the cutoff value can be future candidates for intensive blood pressure lowering and hemostatic therapies in the hyperacute stage of ICH.

This study has several limitations. First, this study was a single-center retrospective study with a small sample size and variable number and timing of follow-up CT scans. Therefore, selection bias may exist and the results may not be generalizable to other populations. Because this study is merely hypothesis generating, further larger cohort studies are needed to validate our present findings. Second, in the comparisons of ROC curves and AUC of multiple models, the Bonferroni correction was not applied because of the small sample size. Third, although we adopted a 10-ml criterion to dichotomize ICH volume based on previous studies, the definition of small ICHs was still vague [3, 19]. Fourth, the volumes of hematoma in our study might be different from those in previous studies using the ABC/2 method. Fifth, despite our effort to lower the systolic blood pressure under 140 mm Hg in order to prevent the HE, the achieved blood pressure and medication regimen for each patient might have been inconsistent. Sixth, the use of reversal agent might affect the relationship between NCCT markers and HE, although the number of cases was small.

## Conclusions

In conclusion, qualitative NCCT markers were less frequently observed in small ICHs in our study. Heterogeneous density and irregular shape were associated with HE in small ICHs. Notably, hematoma density, a quantitative NCCT marker, was associated with HE, regardless of the hematoma volume. Thus, the hematoma size-related difference of NCCT markers needs to be considered in clinical practice, and hematoma density may provide additional use in predicting HE in patients with small ICHs.

## Supplementary Information

The online version contains supplementary material available at <https://doi.org/10.1007/s12028-021-01347-5>.

## Author details

<sup>1</sup> Department of Neurology, Seoul National University Bundang Hospital, Seongnam, Republic of Korea. <sup>2</sup> Department of Neurology, Chungbuk National University Hospital, Cheongju, Republic of Korea. <sup>3</sup> Department of Neurosurgery, Seoul National University Bundang Hospital, Seongnam, Republic of Korea.

## Author contributions

H.-G.J. contributed to the study conceptualization, design, and provided supervision. Y.S.K. and H.-Y.C. performed the statistical analysis, and drafted the article. B.J.K., S.-U.L., J.K., and T.K. contributed to data acquisition and interpretation. H.-J.B., J.S.B., and C.W.O. provided critical review and feedback of the article. M.-K.H. and provided scientific support and critically revised the article. All authors have approved of the final manuscript.

## Funding

This study was supported by the National Research Foundation of Korea (NRF) funded by the Ministry of Science and ICT (Grant #NRF-2020M3E5D9079768).

## Conflicts of interest

No relevant conflict of interest that relates to the research described in this article.

## Ethical approval

This study was performed under ethical research guidelines at Seoul National University Bundang Hospital. The institutional review boards of Seoul National University Bundang Hospital approved this study (approval number: B-2011/648–105).

## Publisher's Note

Springer Nature remains neutral with regard to jurisdictional claims in published maps and institutional affiliations.

Received: 13 April 2021 Accepted: 1 September 2021

Published: 29 September 2021

## References

1. Kazui S, Naritomi H, Yamamoto H, Sawada T, Yamaguchi T. Enlargement of spontaneous intracerebral hemorrhage. Incidence Time Course Stroke. 1996;27:1783–7.
2. Brott T, Broderick J, Kothari R, et al. Early hemorrhage growth in patients with intracerebral hemorrhage. Stroke. 1997;28:1–5.
3. Barras CD, Tress BM, Christensen S, et al. Density and shape as CT predictors of intracerebral hemorrhage growth. Stroke. 2009;40:1325–31.
4. Davis SM, Broderick J, Hennerici M, et al. Hematoma growth is a determinant of mortality and poor outcome after intracerebral hemorrhage. Neurology. 2006;66:1175–81.

5. Broderick JP, Diringer MN, Hill MD, et al. Determinants of intracerebral hemorrhage growth: an exploratory analysis. *Stroke*. 2007;38:1072–5.
6. Wada R, Aviv RI, Fox AJ, et al. CT angiography “spot sign” predicts hematoma expansion in acute intracerebral hemorrhage. *Stroke*. 2007;38:1257–62.
7. Hemphill JC, Besmertis L, Manley GT, Johnston SC. The ICH score: a simple, reliable grading scale for intracerebral hemorrhage. *Stroke*. 2001;32:891–7.
8. Roh DJ, Albers DJ, Magid-Bernstein J, et al. Low hemoglobin and hematoma expansion after intracerebral hemorrhage. *Neurology*. 2019;93:e372–80.
9. Morotti A, Boulouis G, Dowlatshahi D, et al. Standards for detecting, interpreting, and reporting noncontrast computed tomographic markers of intracerebral hemorrhage expansion. *Ann Neurol*. 2019;86:480–92.
10. Bar Y, Diamant I, Wolf L, Greenspan H. Deep learning with non-medical training used for chest pathology identification. *Proc. SPIE 9414, Medical Imaging 2015: Computer-Aided Diagnosis*, 94140V. (2015). Available from <https://doi.org/10.1117/12.2083124>.
11. Yu Z, Zheng J, Li M, et al. Determining the optimal shape-related indicator on noncontrast computed tomography for predicting hematoma expansion in spontaneous intracerebral hemorrhage. *World Neurosurgery*. 2019;121:e584–8.
12. Blacquiére D, Demchuk AM, Al-Hazzaa M, et al. Intracerebral hematoma morphologic appearance on noncontrast computed tomography predicts significant hematoma expansion. *Stroke*. 2015;46:3111–6.
13. Boulouis G, Morotti A, Brouwers HB, et al. Noncontrast computed tomography hypodensities predict poor outcome in intracerebral hemorrhage patients. *Stroke*. 2016;47:2511–6.
14. Delcourt C, Zhang S, Arima H, et al. Significance of hematoma shape and density in intracerebral hemorrhage: the intensive blood pressure reduction in acute intracerebral hemorrhage trial study. *Stroke*. 2016;47:1227–32.
15. Cai J, Zhu H, Yang D, et al. Accuracy of imaging markers on noncontrast computed tomography in predicting intracerebral hemorrhage expansion. *Neurol Res*. 2020;42:973–9.
16. Li Q, Yang WS, Shen YQ, et al. Benign intracerebral hemorrhage: a population at low risk for hematoma growth and poor outcome. *J Am Heart Assoc*. 2019;8:e011892.
17. Behrouz R, Misra V, Godoy DA, et al. Clinical course and outcomes of small supratentorial intracerebral hematomas. *J Stroke Cerebrovascular Dis Official J Natl Stroke Assoc*. 2017;26:1216–21.
18. Dowlatshahi D, Smith EE, Flaherty ML, et al. Small intracerebral haemorrhages are associated with less haematoma expansion and better outcomes. *Int J Stroke Official J Int Stroke Soc*. 2011;6:201–6.
19. Dowlatshahi D, Yogendrakumar V, Aviv RI, et al. Small intracerebral hemorrhages have a low spot sign prevalence and are less likely to expand. *Int J Stroke Official J Int Stroke Soc*. 2016;11:191–7.
20. Li Q, Zhang G, Xiong X, et al. Black hole sign: novel imaging marker that predicts hematoma growth in patients with intracerebral hemorrhage. *Stroke*. 2016;47:1777–81.
21. Shimoda Y, Ohtomo S, Arai H, Okada K, Tominaga T. Satellite Sign: A poor outcome predictor in intracerebral hemorrhage. *Cerebrovasc Dis*. 2017;44:105–12.
22. Flibotte JJHN, O'Donnell J, Greenberg SM, Rosand J. Warfarin, hematoma expansion, and outcome of intracerebral hemorrhage. *Neurology*. 2004;28:1059–64.
23. Brouwers HB, Greenberg SM. Hematoma expansion following acute intracerebral hemorrhage. *Cerebrovasc Dis*. 2013;35:195–201.
24. Jeong HG, Bang JS, Kim BJ, Bae HJ, Han MK. Hematoma Hounsfield units and expansion of intracerebral hemorrhage: a potential marker of hemostatic clot contraction. *Int J Stroke*. 2021;16:163–71.
25. Bergström MEK, Levander B, Svendsen P, Larsson S. Variation with time of the attenuation values of intracranial hematomas. *J Comput Assist Tomogr*. 1977;1(1):57–63.
26. Kim OV, Litvinov RI, Alber MS, Weisel JW. Quantitative structural mechanobiology of platelet-driven blood clot contraction. *Nat Commun*. 2017;8:1274.
27. Tutwiler V, Litvinov RI, Lozhkin AP, et al. Kinetics and mechanics of clot contraction are governed by the molecular and cellular composition of the blood. *Blood*. 2016;127:149–59.
28. Cines DB, Lebedeva T, Nagaswami C, et al. Clot contraction: compression of erythrocytes into tightly packed polyhedra and redistribution of platelets and fibrin. *Blood*. 2014;123:1596–603.
29. Balagurunathan Y, Schabath MB, Wang H, Liu Y, Gillies RJ. Quantitative imaging features improve discrimination of malignancy in pulmonary nodules. *Sci Rep*. 2019;9:8528.
30. Zhan C, Chen Q, Zhang M, et al. Radiomics for intracerebral hemorrhage: are all small hematomas benign? *Br J Radiol*, p 20201047 (2020).